

Electron Energy-Loss and Ultraviolet-Reflectivity Spectra of Crystalline ZnO

R. L. Hengehold and R. J. Almassy*

Air Force Institute of Technology, Wright-Patterson Air Force Base, Ohio 45433

and

F. L. Pedrotti

Aerospace Research Laboratories, Wright-Patterson Air Force Base, Ohio 45433

(Received 3 November 1969)

A comparison between the ultraviolet-reflectivity spectrum and the characteristic energy-loss spectrum of ZnO has been carried out. Reflectivity measurements made over an energy range of band gap to 22 eV yielded a spectrum with structure at 3.34, 5.0, 7.3, and 8.4 eV, and in the region 11–15 eV. Energy-loss measurements made over the energy range of band gap to 50 eV using 10-keV electrons exhibited peaks at 3.82, 5.47, 9.56, 13.5, 18.8, and 35.5 eV. The dominant peak in this spectrum is that at 18.8 eV and has been associated with a plasmon excitation. The samples in both cases were hexagonal ZnO platelets at room temperature. A dispersion analysis has been performed on the reflectivity data yielding the optical constants n , k , ϵ_1 , ϵ_2 , the effective number of free electrons n_{eff} , the effective dielectric constant $\epsilon_{0\text{eff}}$, and the imaginary part of ϵ^{-1} . The energy-loss function has been calculated and found to compare well with the energy-loss spectrum obtained from the electron-transmission measurements.

I. INTRODUCTION

During the last decade, optical-reflectivity measurements have been made on several II-VI compounds^{1–4} in order to determine the higher-energy band structure. Although many edge measurements on ZnO exist,^{5,6} no higher-reflectivity spectrum has been published for this compound. Recently, a theoretical calculation of the band structure of ZnO has been performed by Rössler⁷ using the Korringa-Kohn-Rostoker (KKR) method. This calculation indicates that the major structure in ZnO should occur at energies greater than 10 eV. One of the principal experimental methods used for determining the higher-energy transitions is that of optical reflectivity. Using such data and the Kramers-Kronig dispersion relations, one can calculate the optical constants n and k and the dielectric constants ϵ_1 and ϵ_2 . Either pair of these constants completely describes the optical properties of the system. At ordinary wavelengths, for example, in the visible, these constants may be determined simultaneously by measuring the reflectance of polarized light at oblique incidence. However, if an extended region of photon energies is to be examined, this method is not feasible unless a highly polarized source of vacuum ultraviolet light such as synchrotron radiation is available. If such a source is not available, it is far easier to measure the reflectance at normal incidence and then use dispersion relations to deduce the optical constants.

A second technique which can be applied to determine the higher-energy structure is that of electron-beam spectroscopy. This technique provides

an energy-loss curve over the energy range of interest. The energy-loss function which this curve represents can be shown to be a measure of the imaginary part of the reciprocal dielectric constant. Thus the data obtained from energy-loss measurements can be correlated to that obtained from reflectivity measurements using the dispersion relations.

It should be emphasized that the two external disturbances in question correspond, respectively, to transverse and longitudinal electric fields. Thus the dielectric constants obtained from the two techniques represent two different functions ϵ_L and ϵ_T describing, respectively, the response to longitudinal and transverse external disturbances. In the long-wavelength limit, these two functions are equivalent. Actual measurements are usually made over a photon energy range extending to approximately 25 eV, which is sufficient to determine many of the interesting properties of the elementary excitations of the valence electrons. Since the wavelengths of such photons are much greater than the interionic distances in the crystal, such measurements are assumed to approximate the long-wavelength limit and a direct comparison of the results of these two experiments can be made.

The value of examining the higher-energy excitation spectrum using both techniques has been pointed out by Raether.⁸ Reflectivity measurements show strong peaks near the regions of interband transitions; however, the plasmon energy occurs in a region of very low reflectivity. This energy must be obtained using dispersion analysis which

necessarily involves approximations. The energy-loss curve on the other hand exhibits a large peak at the plasmon excitation energy, but the interband transition peaks are considerably diminished in size. Furthermore, energy-loss measurements can rather easily be extended to energies as high as 50 or 100 eV, whereas reflectivity measurements are difficult at such high energies owing to source problems. Utilization of both techniques provides a more complete picture of the higher-energy structure and optical properties of a material.

This study presents measurements of the reflectivity of ZnO single crystals over the energy range of band gap to 21 eV, and energy-loss measurements of ZnO over the range 0–50 eV. The reflectivity measurements were made at room temperature on hexagonal ZnO crystals in the as-grown condition. These crystals were grown from the vapor phase and were in platelet form. The thickness of the platelets varied from less than $\frac{1}{2} \mu$ to several μ . Crystals grown by this technique⁹ have excellent clear flat surfaces and have been shown to exhibit well-defined exciton structure⁵ and lasing properties.¹⁰ The energy-loss measurements were made on the thinnest of these platelets at room temperature using 10-keV electrons. A dispersion analysis has been performed on the reflectivity data yielding the optical constants n , k , ϵ_1 , ϵ_2 , the effective number of free electrons n_{eff} , the effective static dielectric constant $\epsilon_{0\text{eff}}$, and the imaginary part of ϵ^{-1} . The energy-loss function has been calculated from $\text{Im}(\epsilon^{-1})$ and compared with the energy-loss spectrum obtained from the electron-transmission measurements.

II. REFLECTIVITY MEASUREMENTS

Reflectivity measurements were made using a 1-m Jarrel-Ash vacuum ultraviolet monochromator (Seya mount) fitted with a reflection chamber similar to that described by Cardona.¹ A Tanaka-type discharge lamp with 60-cps ac excitation and a source gas of hydrogen was used as the light source from 1000 to 4000 Å. The line spectrum of hydrogen was used up to 1650 Å. Above this the continuous spectrum of hydrogen permitted reflectivity measurements at regular intervals of 10 Å. Below 1000 Å, a supported dc discharge was used employing argon, helium, and nitrogen as source gases. The measurements above 1000 Å were made using a 30 000-lines-per-in. grating blazed at 1100 Å and overcoated with MgF_2 . Below 1000 Å, a grating overcoated with gold was used. The reflectivity attachment is designed so that detection of both incident and reflected light could be accomplished using the same 1P21 multiplier. A coating of sodium salicylate on the glass window of the

multiplier allowed detection into the far vacuum ultraviolet. All measurements reported here were taken at room temperature. The angle of incidence used for these measurements was approximately 15° . Since the variation of the reflectivity from that at normal incidence is very small for angles up to 15° ,¹¹ these measurements were assumed to satisfy the normal incidence requirement. No efforts were made to polarize the incident light, however, as is well known, the light from a Seya monochromator does contain a slight degree of polarization. This is not believed to have been sufficient to have affected the reflectivity curve presented here since the variation observed between spectra taken from platelets oriented in different directions was within the limits of error of the measurements.

The reflectivity spectrum obtained for ZnO is shown in Fig. 1. The relative accuracy of the measurements is approximately $\pm 5\%$ below 12 eV and $\pm 10\%$ above 12 eV. The increase in the error above 12 eV is due to fluctuations in the line source used in this region. The low-energy limit of the data was determined by the onset of strong reflection from the back surface of the thin ZnO platelet at energies below the fundamental absorption edge of 3.34 eV. Reflectivities below this energy were calculated using direct measurements of the index of refraction¹² and an exponential extrapolation to the reflectivity at zero energy. The curve between the absorption edge and 8 eV was obtained from data taken every 10 Å, whereas that above 8 eV was obtained using the line spectra of several gases. As a result, the resolution below 8 eV is con-

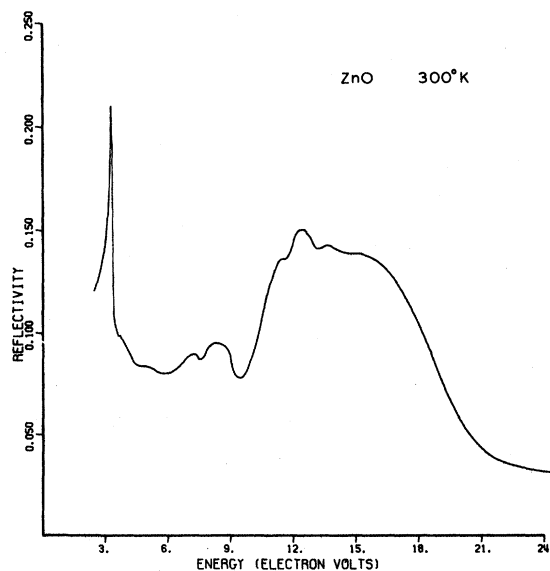


FIG. 1. Near-normal incidence reflectivity spectrum typical of a platelet of ZnO at 300 °K.

siderably better than in the region 8–22 eV, and, in fact, sharp structure above 15 eV could have been missed due to energy gaps in the source lines available. Beyond 22 eV, the reflectivity was fit to a smooth reciprocal power function chosen according to $R(E) = CE^{-4}$.

The reflectivity of ZnO is not, in general, that exhibited by other IIB-VIA compounds^{1,2} in that the major structure begins beyond 10 eV, whereas in the other IIB-VIA compounds such as CdS, CdSe, and ZnS the valence-band transitions are practically exhausted at this energy and the reflectivity is on a sharp decrease. This would seem to indicate that the valence bands in ZnO lie considerably lower than those of the other IIB-VIA compounds.

Analysis of the data obtained in this experiment involves the use of the Kramers-Kronig integrals. These dispersion integrals and the various relationships which result from them have been developed in detail elsewhere.¹³ The curves for the real and imaginary parts of the complex refractive index n and k are shown in Fig. 2. The behavior of k indicates strongest absorption at the edge and above 10 eV. The low-energy absorption compares well with the direct-absorption measurements of ZnO films made by Heiland, Mollwo, and Stockmann.¹⁴ The real and imaginary parts of the complex dielectric constant are shown in Fig. 3. The maxima of ϵ_2 , associated with single-particle excitations, show predominant transitions at the edge (3.34 eV), at 5.0, 7.3, and 8.4 eV and in the region 11–13 eV. Structure in this last region

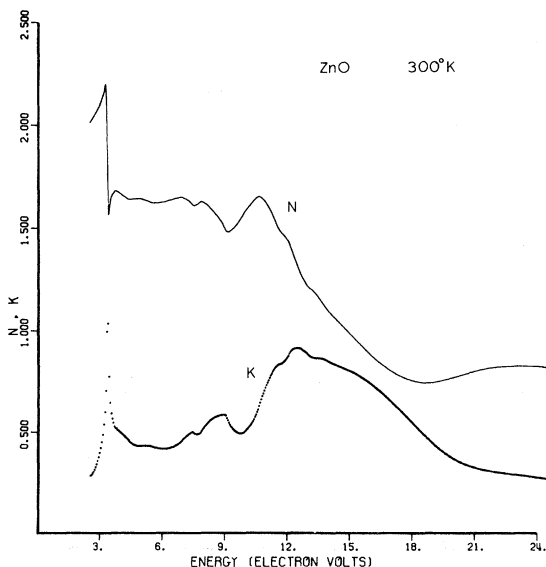


FIG. 2. Optical constants n and k of ZnO computed via a Kramers-Kronig analysis of the reflectivity spectrum of Fig. 1.

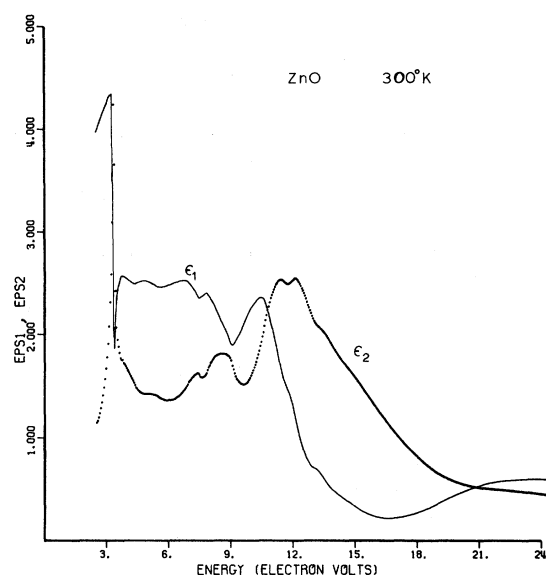


FIG. 3. Dielectric constants ϵ_1 and ϵ_2 of ZnO computed via a Kramers-Kronig analysis of the reflectivity spectrum of Fig. 1.

cannot be well resolved due to an absence of a continuum source at these energies.

Some insight into the processes occurring in the solid can be obtained from the values of $\epsilon_{0\text{eff}}$ and n_{eff} . These two quantities have been derived and discussed by Ehrenreich and Phillip. The first of these, the effective dielectric constant, can be calculated from

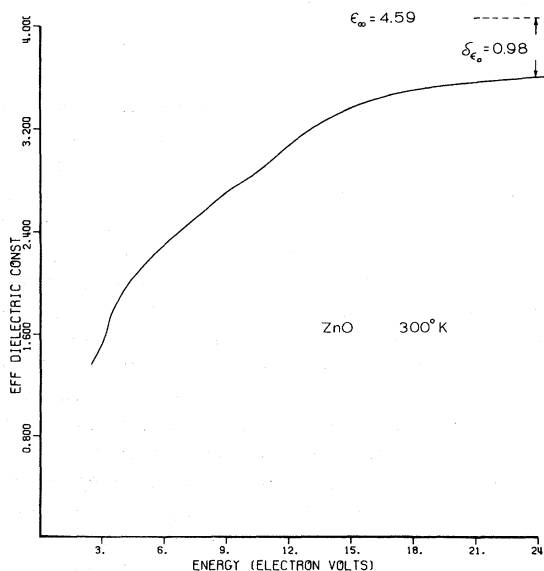


FIG. 4. Effective dielectric constant $\epsilon_{0\text{eff}}$ of ZnO. The high-frequency dielectric constant is shown by the dashed-line segment.

$$\epsilon_{0\text{eff}}(\omega_0) = 1 + (2/\pi) \int_0^{\omega_0} \omega^{-1} \epsilon_2(\omega) d\omega. \quad (1)$$

The result of this calculation for ZnO is shown in Fig. 4. The difference between $\epsilon_{0\text{eff}}$ at the high-frequency end of the data and the value obtained by direct measurement of the high-frequency dielectric constant is called $\delta\epsilon_0$ by Ehrenreich and Phillip.¹³ In the case of ZnO, this difference is found to be 0.98. Such a substantial difference suggests the possibility that further structure in the reflectivity may be present beyond the energy range measured, i. e., beyond 22 eV. Similarly, the effective number of free electrons taking part in the excitations up to the limit of the data can be calculated from

$$n_{\text{eff}}(\omega_0) = (m/2\pi^2 Ne^2) \int_0^{\omega_0} \omega \epsilon_2(\omega) d\omega, \quad (2)$$

where N is the atom density of the crystal. The result of this calculation for ZnO is shown in Fig. 5. It is somewhat surprising to find that n_{eff} is only approaching a value of two electrons per atom at a photon energy of above 20 eV. The computer program used for this calculation has been used on reflectivity data of III-V compounds, and in this case does indeed yield a value of n_{eff} greater than four at these energies. The deficiency in the calculated value of n_{eff} is at least consistent with the low value of $\epsilon_{0\text{eff}}$, again implying high-energy structure beyond that measured, which could contribute to the integral. It should be noted that n_{eff} increases smoothly and gives no indication that it is beginning to level off. A gradual leveling

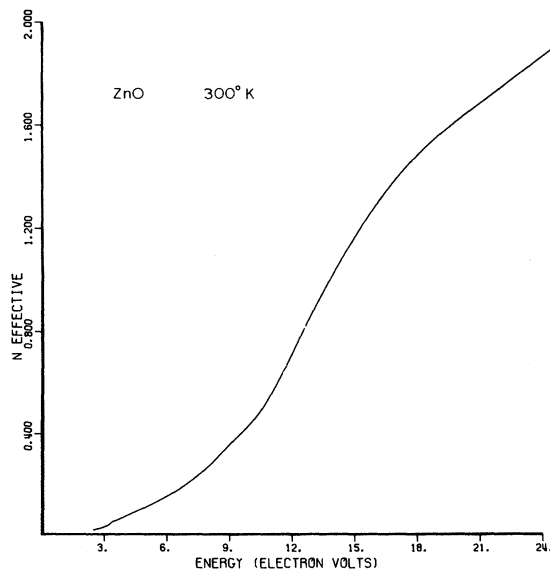


FIG. 5. Effective number of electrons n_{eff} taking part in the interaction.

off would be expected as the sum rule becomes exhausted. The smooth increase gives no hint that the onset of d -band transitions has been reached. Furthermore, one would expect possible d bands just beyond these energies to contribute to ϵ_2 in the region shown due to coupling with the valence bands. For the III-V compounds investigated by Ehrenreich and Phillip,¹³ such coupling led to a definite rise in n_{eff} above the value of four, even before transitions from the d bands were energetically possible. Thus, it appears that in the case of ZnO further structure is present at higher energies which is not attributable to d bands. In fact, values of $n_{\text{eff}} < 2$ imply that the oxygen 2s electrons have not yet made their contribution and as a result lie very deep. Such an interpretation would receive support from the theoretical orthogonalized-plane-wave (OPW) calculations of Stukel *et al.*,¹⁵ which show the s bands in ZnS lying more than 1 Ry below the conduction band. Since the major valence structure in ZnO occurs at higher energies than that in ZnS, these theoretical results would imply that the oxygen s bands in ZnO lie even deeper than they do in ZnS.

These tentative conclusions would, however, seem to be at variance with the recent KKR calculations performed by Rössler.⁷ Although those calculations predict the general characteristics of the reflection spectrum obtained here they show the d bands to be quite broad (1.6 eV) and to lie only 4 eV below the top of the valence band. Thus the d electrons would contribute to the large broad peak at 15 eV and necessarily raise the value of n_{eff} above that obtained here.

III. ENERGY-LOSS MEASUREMENTS

The electron energy-loss measurements were performed using an apparatus similar to that described by Blackstock, Birkhoff, and Slater¹⁶ and by Marton and Simpson.¹⁷ It consists of an electron gun, sample holder, electron decelerator, energy analyzer, and electron multiplier. These components are contained in a demountable glass vacuum system employing copper-gasketed seals and a zeolite trap to avoid organic contamination.

Figure 6 is a simplified schematic of the apparatus. The electron gun is of the Steigerwald type with a tungsten hairpin filament. This gun produces a well-collimated beam of 10-keV monoenergetic electrons. The filament was biased 100 V below ground and thus the electrons reach the sample with 10 100 eV of energy. After passing through the sample, the electrons are decelerated through 10 keV using the same power supply as that used for acceleration. In this way, any fluctuations in the power supply have no effect on the measurements. The decelerator was construc-

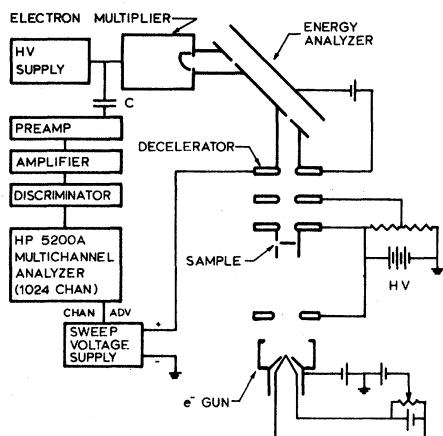


FIG. 6. Schematic of the apparatus used for the electron energy-loss measurements.

ted using the design of Mendlowitz,¹⁸ which provides for deceleration in the axial direction without introducing any radial changes. The analyzer itself is a parallel-plate electrostatic type similar to that described by Harrower.¹⁹ The entrance and exit slits of this analyzer are rectangular in shape, 0.007 in. wide, 0.25 in. long, and spaced 2 in. apart. Such an analyzer will provide a resolution of slightly less than 1%. The measured resolution of the system was 0.75%, so that, in this case, energy losses differing by 0.75 eV could be resolved. Electrons leaving the analyzer entered a secondary emission multiplier (14 stage, BeCu dynodes), the first dynode of which was carefully shielded against collection of stray electrons. The output pulses from the multiplier were amplified and shaped, and then recorded using a Hewlett Packard 5200A multichannel analyzer (MCA) in the multiscalar mode.

Electron energy distributions were observed by sweeping the voltage on the final decelerator plate, while keeping the voltage between the energy analyzer plates fixed to pass 100-eV electrons. The sweep voltage is obtained from the channel advance of the MCA. This voltage is amplified using a Kepco ABC 200 programmable power supply. Two sweep ranges have been used in this study, 0–25.6 and 0–51.2 V. Electrons which have lost no energy in passing through the sample will arrive at the analyzer with 100 eV of energy and pass through the analyzer when the sweep voltage is at 0 V, whereas electrons which have suffered energy losses between 0 and 51.2 eV will pass through at various sweep voltages. The choice of a sweep of 0–51.2 eV provides the x axis of the MCA display with 0.05 eV/channel. The y axis of the display represents the number of electrons which have lost any particular energy, and thus one immediately obtains a plot of the energy-loss function.

Sweep speeds of approximately 100 msec/channel were used in this study. Data acquisition was continued until sufficient data were collected to provide a good statistical representation. Run times vary from 10 min to several hours, depending on the beam density and sample thickness.

The sample holder allows accurate positioning of the sample on the axis of the electron optical system and the sample can be removed from the beam for alignment purposes. The samples used in this study were very thin ($< 0.5 \mu$) ZnO platelets in the as-grown condition which provided considerably more detailed structure than evaporated thin films of ZnO. The data reported here is that obtained from two different platelets.

The energy-loss spectrum obtained for ZnO is shown in Fig. 7. The peaks present in this curve are at 3.8, 5.5, 9.5 eV, a shoulder at 13.5 eV, a large dominant peak at 18.8 eV, a small shoulder at 22 eV, and a small plateau-like structure at 35.5 eV. By comparing the energy-loss results with the optical results, particularly ϵ_1 and ϵ_2 , the type of excitation responsible for the various peaks can be determined. In general, such peaks can be associated with interband transitions or plasmon excitations. A true plasmon excitation will exhibit a large peak in the energy-loss spectrum with corresponding values of ϵ_1 and ϵ_2 which are near zero. An interband transition, on the other hand, will be marked by small structure in the energy-loss spectrum with corresponding values of ϵ_1 and ϵ_2 which are nonzero. The exact value of ϵ_1 and ϵ_2 for such a transition depends upon the strength of the transition. On this basis, the first three peaks

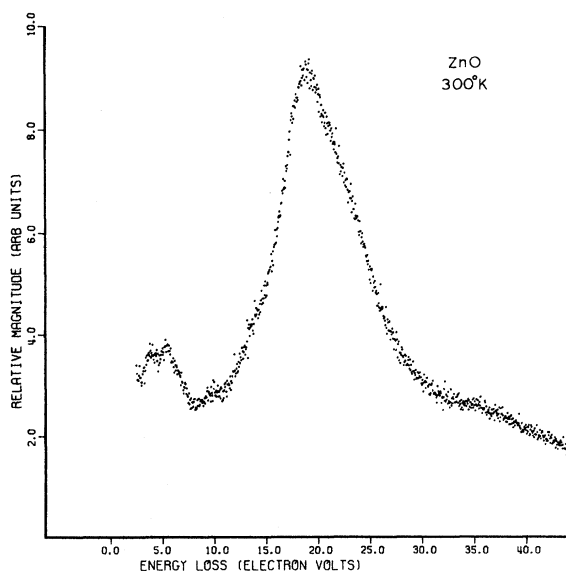


FIG. 7. Energy-loss spectrum of a typical ZnO platelet.

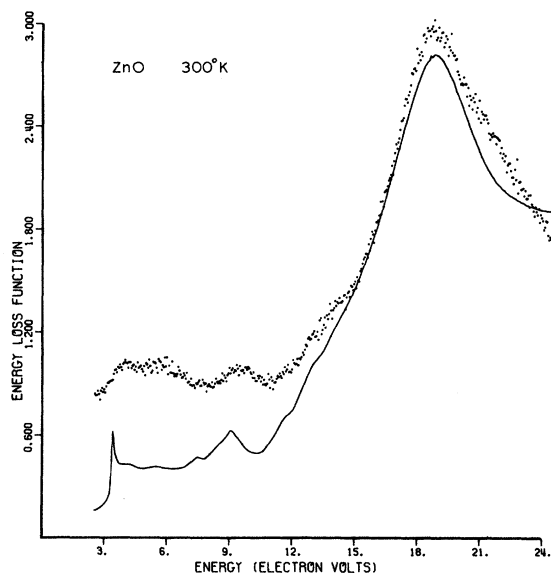


FIG. 8. Energy-loss function of ZnO as computed from reflectivity data is shown by the solid curve. The dotted curve shows the energy-loss data which has been normalized to the value of the energy-loss function at the plasma energy.

and the shoulder at 13.5 eV can be associated with valence-band transitions. This structure does not appear as sharp as that observed in the reflectivity spectrum owing to the decreased resolution of this type of experiment and the decrease in peak height because of the functional behavior of $\text{Im } \epsilon^{-1}$. The large dominant peak at 18.8 eV can be associated with a single plasmon excitation. This peak is unsymmetrical with a shoulder at 13.5 eV (also see Fig. 8) and indications of a small shoulder at 22.0 eV. It does appear clear that interband transitions are present near the plasma peak which would account for its nonsymmetrical nature. The plateau in the region of 35 eV could be due either to an interband transition such as would result from d -band excitation or from a double-plasmon event.

Comparison of the results of reflectivity measurements with those obtained from energy-loss measurements requires an expression for the cross section for electron interaction in a thin crystal. Hubbard²⁰ has considered this problem and has developed an expression for the probability of an electron interaction which will result in the probe electron being scattered through an angle θ ($0 < \theta < \theta_0$) and losing energy $\hbar\omega$. The expression takes the form

$$\frac{d\sigma}{dE} = \frac{me^2}{2\pi\hbar E_0} (\text{Im } \epsilon^{-1}) \ln \left(\frac{\theta_0^2 + \theta_E^2}{\theta_E^2} \right), \quad (3)$$

where σ is the cross section for this type of scat-

ter, E_0 is the initial energy of the probe electron, $\theta_E = \hbar\omega/mv^2 = \Delta E/2E_0$, and θ_0 is an equipment parameter. This development shows that the characteristic energy-loss spectrum obtained will be a function not only of the imaginary part of the inverse dielectric constant but also of θ_0 and θ_E . The parameter θ_0 which represents the maximum angle of scatter possible in the experimental system, was determined to be approximately 2 mrad in this case. The results of this calculation are shown in Fig. 8 along with the experimentally obtained energy-loss data. As can be seen from these curves the over-all agreement is quite good; however the higher resolution of the optical measurements at energies below 10 eV permits more detailed structure in the calculated function.

If the loss at 18.8 eV is due to collective excitation of the valence electrons, the theoretical plasma frequency can easily be estimated from the expression for the free-electron plasma frequency

$$\omega_p = (4\pi ne^2/m)^{1/2}, \quad (4)$$

where n is the free-electron density in the material and m is the electronic mass. If four free electrons are assumed, $\hbar\omega_p$ is equal to 21.5 eV; however if three free electrons are assumed, $\hbar\omega_p$ is 18.7 eV. This simple calculation would indicate that only the 4s electrons of zinc and the 2p electrons of oxygen are taking part in the plasma oscillation. This implies that the 2s electrons of oxygen are indeed lying quite deep in energy and do not enter into this effect. Such an interpretation would agree with that discussed earlier in Sec. II. On the other hand, the observed position of the plasma peak could be a result of a shift of the free-electron peak owing to nearby interband transitions. Wilson²¹ has considered the effect of such interband transitions on the free-electron plasma energy. His results indicate that a broad band just below the plasma peak would cause the free-electron peak to be shifted to higher energies, whereas a narrow band just above the plasma peak would cause the free-electron peak to be shifted to lower energies. Since the data in the present experiment indicate the existence of a broad fairly strong absorption band just below the plasma peak, the conclusion might be reached that the observed plasma peak occurs at an energy which is higher than that of the true free-electron peak. Such a conclusion would imply that $\omega_p < 18.8$ eV and thus that $n < 3$, a result which would tend to agree more closely with the optical value of n_{ext} . However, the present data also indicate that interband transitions such as d - or $2s$ -band excitations probably occur above the plasma peak. That such transitions are not observable in the optical data is possibly due to the fact that they lie above 22 eV or

enter as sharp peaks not observed due to the poor resolution available in this region of the reflectivity spectrum. The nonsymmetrical nature of the plasma peak would indicate the existence of such transitions. The presence of such transitions could act to shift the free-electron plasma peak to lower energies. Thus in the case of the present experiment, the effect of nearby interband transitions on the plasma peak is not clear.

It should be pointed out that if interband transitions do occur in the region near 20 eV as is evidenced by the nonsymmetrical nature of the plasma peak, the smooth extrapolation used in the Kramers-Kronig calculations is not entirely justified and the calculation of n_{eff} could be incorrect since it assumes that the f sum for the valence electrons has been exhausted. Since n_{eff} does not level out at the highest energies considered, this assumption is probably in error and no clear interpretation of n_{eff} can be made. On the other hand, the value of n obtained from the energy-loss curve, i. e., three free electrons, should be meaningful. Such a low value of n would again indicate that neither the 2s electrons of oxygen nor the d electrons of zinc are involved. Until more detailed data are available in the region above 20 eV, however, a smooth extrapolation appears to be the only reasonable approach to this calculation.

IV. CONCLUSIONS

A correlation has been made between the data obtained from an optical-reflectivity measurement and an electron energy-loss measurement on ZnO. The reflectivity measurements were made over the energy range 3–22 eV and the energy-loss measurements over the energy range 3–50 eV. The correlation was accomplished by use of a Kramers-Kronig analysis of the reflectivity data. The results obtained indicate that the reflectivity spectrum of ZnO differs considerably from that of other II-VI compounds in that the major interband transitions occur at energies beyond 10 eV.

The results obtained from the Kramers-Kronig analysis indicate that some of the four so-called valence electrons lie very deep in energy as do the zinc d electrons. The effective number of free electrons n_{eff} has a value of approximately two at energies > 20 eV, and the number of free electrons taking part in the plasma oscillation is approximately three. Thus it appears as if the 2s electrons of oxygen and the d electrons of zinc lie very deep in energy in ZnO, a fact which could possibly be due to the ionic character of this compound. The precise interpretation of n_{eff} is not entirely clear in this case, since interband transitions probably exist at energies higher than 20 eV and have not been included in the integral. However, it is very doubtful that the value is in error by the two electrons required to raise it to four. It is even more doubtful that the d bands have made a contribution, since this would require a value of n_{eff} greater than four. The discrepancy with Rössler's band calculations which predict a strong contribution from the d electrons remains to be clarified. In this regard, a calculation of the joint density of states for Rössler's energy bands would be helpful.

The above question could better be resolved if reflectivity measurements were made beyond 22 eV with good resolution. Furthermore, polarized measurements in the vacuum ultraviolet will help in the assignment of the various valence-band transitions observed in the data. Park²² has made preliminary measurements of ZnO using synchrotron radiation. However, although these measurements show polarization dependence and greater resolution, they basically differ little from those presented here.

ACKNOWLEDGMENTS

The authors wish to thank R. Euwema and T. C. Collins for their helpful discussions concerning the interpretation of the results, and J. Gilbert for his help in making the measurements of reflectivity.

*Present address: Physics Department, U.S. Air Force Academy, Colorado Springs, Colo.

¹M. Cardona and G. Harbeke, Phys. Rev. **137**, A1467 (1965).

²R. Hengehold and C. Fraime, Phys. Rev. **174**, 808 (1968).

³D. M. Roessler and W. C. Walker, Phys. Rev. **159**, 733 (1968).

⁴D. M. Roessler and W. C. Walker, J. Phys. Chem. Solids **30**, 157 (1969).

⁵Y. S. Park *et al.*, Phys. Rev. **143**, 512 (1966).

⁶D. G. Thomas, J. Phys. Chem. Solids **15**, 86 (1960).

⁷U. Rössler, Phys. Rev. **184**, 733 (1969).

⁸H. Raether, in *Springer Tracts in Modern Physics*, edited by G. Hohler *et al.* (Springer, Berlin, 1965), Vol. 38, p. 85.

⁹Y. S. Park and D. C. Reynolds, J. Appl. Phys. **38**, 756 (1967).

¹⁰F. H. Nicoll, Appl. Phys. Letters **9**, 13 (1966).

¹¹D. L. Greenaway and G. Harbeke, *Optical Properties*

and *Band Structure of Semiconductors* (Pergamon, New York, 1968), p. 25.

¹²Y. S. Park and J. R. Schneider, *J. Appl. Phys.* **39**, 3049 (1968).

¹³H. R. Phillip and H. Ehrenreich, in *Semiconductors and Semimetals*, edited by R. Willardson and A. Beer (Academic, New York, 1967), Vol. 3, p. 93.

¹⁴G. Heiland, E. Mollwo, and F. Stockmann, in *Solid State Physics*, edited by F. Seitz and D. Turnbull (Academic, New York, 1959), Vol. 8, p. 191.

¹⁵D. Stukel *et al.*, *Phys. Rev.* **179**, 740 (1969).

¹⁶A. W. Blackstock, R. D. Birkhoff, and M. Slater,

Rev. Sci. Instr. **26**, 274 (1955).

¹⁷L. Marton and J. A. Simpson, *Rev. Sci. Instr.* **29**, 567 (1958).

¹⁸H. Mendlowitz, *Rev. Sci. Instr.* **29**, 701 (1958).

¹⁹G. A. Harrower, *Rev. Sci. Instr.* **26**, 852 (1955).

²⁰J. Hubbard, *Proc. Phys. Soc. (London)* **A68**, 976 (1955).

²¹C. B. Wilson, *Proc. Phys. Soc. (London)* **76**, 481 (1960).

²²Y. S. Park *et al.*, DESY Report No. 7019, 1970 (unpublished).

PHYSICAL REVIEW B

VOLUME 1, NUMBER 12

15 JUNE 1970

Self-Consistent Energy Bands and Related Properties of Boron Phosphide

D. J. Stukel

Aerospace Research Laboratories, Wright-Patterson Air Force Base, Ohio 45433

(Received 29 December 1969)

A first-principles self-consistent orthogonalized-plane-wave energy-band calculation has been performed for cubic boron phosphide (BP) using a nonrelativistic formalism and Slater's free-electron exchange approximation. These are the first fully self-consistent energy-band solutions reported for BP. The imaginary part of the dielectric constant, spin-orbit splittings, effective masses, deformation energies, and the x-ray form factors (Fourier transforms of the electron charge density) have been calculated. The theoretical results are compared with the available experimental data.

I. INTRODUCTION

Boron phosphide (BP) is a group III-V compound semiconductor. Scientific interest in this compound is stimulated by its potential for solid-state devices; however, many of the important basic physical properties have not been well established. Crystalline BP, as a substance for semiconductor compounds, has advantages such as a high melting point, chemical inertness, and high mechanical hardness.

Cubic BP has a melting point greater than 3000 °C but decomposes into B₆P and P₂ at much lower temperatures. Hence, the customary methods of crystal growing are not applicable. However, single crystals of sufficient size and purity for optical and electrical measurements have been prepared. Methods of growing crystalline BP have been reviewed by Williams.¹ BP crystallizes in the fcc zinc-blende structure with a lattice parameter of 4.538 Å.^{2,3} BP shows both physical and chemical properties that differ from the general trend of the III-V family. BP is quite inert chemically. It has a hardness about equal to that of SiC.⁴

The purpose of this paper is to report for BP a theoretical calculation of the band structure, the

imaginary part of the dielectric constant (ϵ_2) derived from the theoretical bands, spin-orbit splittings, effective masses, deformation energies, and the form factors (the Fourier transforms of the electron charge density).

In the past couple of years, a great deal of success has been attained in calculating the energy band structures of group III-V, II-VI, and IV compounds using an unadjusted first-principles self-consistent orthogonalized-plane-wave (SCOPW) model developed here at the Aerospace Research Laboratories. The (SCOPW) programs used to calculate the electronic band structure have given surprisingly good one-electron band energies for tetrahedrally bonded compounds when Slater's exchange is used.⁵⁻¹¹

II. CALCULATIONAL DETAILS

A. Self-Consistent OPW model

The orthogonalized-plane-wave (OPW) method of Herring¹² is used to calculate the electron energies. In the SCOPW model,^{5,6} the electronic states are divided into tightly bound core states and loosely bound valence states. The core states must have negligible overlap from atom to atom. They are